Detection and characterization of many-body localization in central spin models

Daniel Hetterich, Norman Y. Yao, Maksym Serbyn, Frank Pollmann, and Björn Trauzettel

Detection and characterization of Many-Body Localization in Central Spin Models

Daniel Hetterich,[1] Norman Y. Yao,[2] Maksym Serbyn,[3] Frank Pollmann,[4] and Björn Trauzettel[1]

[1]*Institute for Theoretical Physics, University of Würzburg, 97074 Würzburg, Germany*
[2]*Department of Physics, University of California, Berkeley, California 94720, USA*
[3]*Institute of Science and Technology, 3400 Klosterneuburg, Austria*
[4]*Department of Physics, Technical University Munich, 85748 Garching, Germany*
(Dated: October 11, 2018)

We analyze a disordered central spin model, where a central spin interacts equally with each spin in a periodic one dimensional random-field Heisenberg chain. If the Heisenberg chain is initially in the many-body localized (MBL) phase, we find that the coupling to the central spin suffices to delocalize the chain for a substantial range of coupling strengths. We calculate the phase diagram of the model and identify the phase boundary between the MBL and ergodic phase. Within the localized phase, the central spin significantly enhances the rate of the logarithmic entanglement growth and its saturation value. We attribute the increase in entanglement entropy to a non-extensive enhancement of magnetization fluctuations induced by the central spin. Finally, we demonstrate that correlation functions of the central spin can be utilized to distinguish between MBL and ergodic phases of the 1D chain. Hence, we propose the use of a central spin as a possible experimental probe to identify the MBL phase.

Introduction.—Many-body localization (MBL) is the interacting analog of Anderson localization [1, 2]. As localized systems are perfect insulators, they violate the eigenstate thermalization hypothesis (ETH) [3, 4]. This violation implies that expectation values of physical observables with respect to eigenstates may not be described by thermodynamic ensembles anymore. Hence, the characteristic repulsion between energy levels of typical thermalizing systems [5] is absent in the MBL phase. The absence of level repulsion and the intrinsic memory about the initial state in the MBL phase may be understood via an emergence of local integrals of motion [6, 7]. ETH can also be violated in systems that do not experience MBL, such as integrable systems [8]. However, in contrast to integrable systems, the MBL phase is stable to weak but finite local perturbations (see [9] for a recent review). Moreover, the signatures of MBL can be observed in presence of weak coupling to heat baths [10] and particle loss [11]. However, the robustness of MBL exposed to long-range interactions is still an open question. While it has been proposed that MBL exists in systems with interactions that decay with distance as a power law [12, 13], in a recent work it is argued that MBL could be present in systems with non-decaying interactions [14].

In this paper, we study the behavior of the MBL transition in the presence of a central spin that equally couples to all other spins in the model [15]. Our model therefore obtains a very particular type of long-range interaction, in which each spin is effectively coupled to all other spins via the central spin. These models are experimentally relevant for spin qubits based on electrons captured in quantum dots [16]. In such systems, a qubit plays the role of the central spin that experiences decoherence due to the environmental bath spins [17–20]. The central spin interacts with the bath of nuclear spins via hyperfine in-

teraction [21, 22] which was experimentally investigated in different host materials [23]. Similarly, nitrogen vacancies in diamond represent central spins whose main source of decoherence are electron spins of surrounding nitrogen impurities [24, 25].

The main result of this work is that a central spin can be employed in order to detect localization of its environment. To this end, we first study the impact of the central spin on the well-known MBL transition of the Heisenberg chain [26, 27]. We find an analytic expression for the critical disorder at which the transition from MBL to the ergodic phase appears. The central spin establishes a non-local coupling that enhances the rate of the logarithmic growth of the half-chain entanglement entropy and its saturation value. We observe that this enhancement has the same form as the non-extensive increase in magnetization fluctuations that we find, which suggests a relation between these two effects. The latter effect was analytically analyzed in a fermionic non-interacting central site model (NCSM) [28]. Finally, we propose a novel detection scheme for MBL based on the autocorrelation function of the central spin. Unlike previous detection schemes [29–32], the central spin is capable of distinguishing between ergodic and localized environments at short times. This feature stems from the large frequency dependency of its autocorrelation function which is qualitatively different in both environmental phases.

Model.—We extend the random field Heisenberg chain showing a MBL transition [26, 27] by coupling all sites to the central spin:

$$H = J \sum_{i=1}^{K} \vec{I}_i \cdot \vec{I}_{i+1} + \sum_{i=1}^{K} B_i I_i^z + \frac{A}{K} \sum_{i=1}^{K} \vec{S} \cdot \vec{I}_i, \quad (1)$$

where $\vec{S} = \frac{1}{2}(\sigma_x, \sigma_y, \sigma_z)^T$ is the central spin that equally couples to the K spins $\vec{I}$ of the Heisenberg chain with
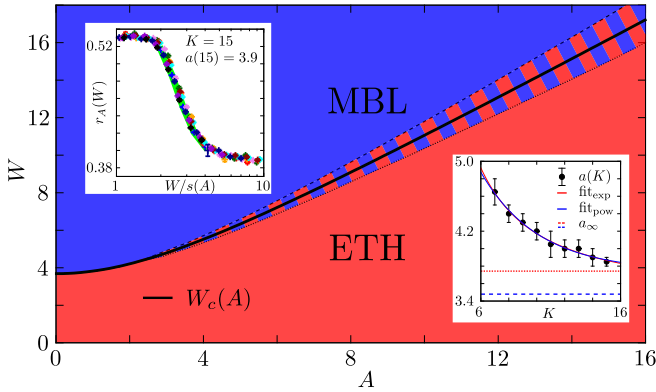
Figure 1. Phase diagram of the central spin model. The critical disorder strength $W_c(A) = s(A) \cdot W_c^{\text{Heis}}$ (solid line), at which the eigenvalues in the center of the band transition from a Poisson distribution towards the GOE ensemble, grows with coupling strength A to the central spin. The stripes represent the uncertainty of the parameter a_∞, which arises from the extrapolation extrapolation of $a(K)$ to the thermodynamic limit, see right inset. We find $a_\infty = 3.55 \pm 0.25$, where the uncertainty arises by comparing power-law or exponential fitting functions. Each value $a(K)$ is obtained by a scaling analysis as illustrated in the left inset, where the disorder strength is rescaled by $s(A)$ for all simulated values of A.

periodic boundary conditions. The random fields B_i are uniformly distributed $B_i \in [-W, W]$, where W sets the disorder strength, and we set $J = 1$ in the following.

For $J = 0$, our model becomes similar to a previously studied system [33], where the l-bit [6, 7] representation of MBL was employed to study the influence of a central spin on its MBL environment. The authors of Ref. [33] demonstrated that the l-bits remain localized when their coupling strength to the central spin is rescaled with the inverse system size. Hence, in Eq. (1) we choose the coupling of the central spin to the physical spin degree of freedoms to be A/K. Such scaling ensures that the spectral bandwidth of the coupling term is independent of system size. Then, the spatially non-local coupling term to the central spin can be considered as being local in energy space. Moreover, a coupling rescaled in this way is experimentally relevant in certain quantum dot models [16, 22], for which we propose below a concrete way to detect MBL. While the relaxation features of similar central spin models have previously been studied [34, 35], we focus on the MBL signatures of central spin models in this paper.

Phase diagram of the central spin model.—An efficient way to distinguish ergodic and localized phases is to exploit their different eigenvalue statistics. While eigenvalues repel each other in the ergodic phase, leading to a Gaussian Orthogonal Ensemble (GOE) of levels, eigenvalues are simply Poisson-distributed (POI) in localized phases. Both phases lead then to different distributions of gaps $g_i = E_{i+1} - E_i$ of adjacent energies. A commonly

used indicator of level statistics is the ratio of adjacent energy gaps, $r_A(W) = \langle \min(g_i, g_{i+1}) / \max(g_i, g_{i+1}) \rangle_i$ [36], which takes values between ≈ 0.53 (GOE) and 0.38 (POI). The average runs over disorder ensembles and eigenvalues in the center of the spectrum. Since the bandwidth of the terms responsible for coupling to the central spin is limited, their effect on the levels E_i of the Heisenberg chain crucially depends on the position in the spectrum. We focus on levels in the center of the band, where the density of states is largest and one expects the onset of delocalization.

In the absence of the central spin, the model is known to show a MBL transition at $W_c(A = 0) = W_c^{\text{Heis}} \approx 3.7$ [26, 27]. Upon increasing A we find that $r_A(W)$ is well approximated by $r_A(W) = r_0(W/s(A))$, where $r_0(W)$ is the value of the indicator r for the pure random field Heisenberg chain. The rescaling function

$$s(A) = \sqrt{1 + (A/a)^2}, \qquad (2)$$

depends on a single parameter a that changes with system size but does not depend on the disorder strength [37]. We predict this functional form of the rescaling function we predict the basis of the limits found in previous works: For small values of A, Eq. (2) recovers the result of the random field Heisenberg chain with a second order correction. This behavior is very similar to the case of the NCSM [28]. On the other hand, for $A \gg 1$ we obtain $W_c(A) \sim A$, consistent with predictions of Ref. [33].

The quality of the rescaling collapse is shown in the left inset of Fig. 1, where the results for many different coupling constants A are mapped onto the known result of the random field Heisenberg chain. The asymptotic value of the free parameter as $K \to \infty$ is determined to be $a = 3.55 \pm 0.25$. The finite size scaling analysis is shown in the right inset of Fig. 1. Finally, Fig. 1 illustrates the resulting critical disorder strength

$$W_c(A) = W_c^{\text{Heis}} s(A), \qquad (3)$$

which separates the localized from the ergodic phase. We want to emphasize that, for a given disorder strength $W > W_c^{\text{Heis}}$, the central spin needs to couple sufficiently strong in order to delocalize eigenstates in the center of the band. This result is a clear many-body effect, because, for the NCSM, we have found an energy window of size $\sim A^2/K$ consisting of repelling eigenvalues at any $A > 0$ [28].

Logarithmic growth of entanglement entropy.— The logarithmic growth of entanglement entropy is employed as a signature of the interacting localized phase with local Hamiltonians [38, 39]. At the same time, the non-local NCSM also displays logarithmic growth of entanglement entropy despite the absence of interactions [28]. Therefore, it is instructive to study the dynamics of entanglement entropy in the interacting central spin model. Starting with the Néel state $|\psi(t = 0)\rangle =$

$| \uparrow\downarrow\uparrow \ldots\rangle$, we compute the reduced density matrix $\rho_{\mathcal{A}} = \mathrm{tr}_{\mathcal{B}} \left[|\psi(t)\rangle\langle\psi(t)| \right]$, where we trace out $K/2$ contiguous spins. As the entanglement entropy is $S_{\mathcal{A}} = S_{\mathcal{B}} = -\mathrm{tr} \left[\rho_{\mathcal{A}} \ln \rho_{\mathcal{A}} \right]$, the result is independent of which bipartition contains the central spin. For coupling strength $A = 0$, we recover the case of a periodic Heisenberg chain. Here, $S_{\mathcal{A}}^{\mathrm{Heis}}(t) \sim \xi s_{\infty} \ln t$ grows logarithmically in time, where ξ is the localization length of the model in the absence of interactions and s_{∞} the contribution to the saturation value of $S_{\mathcal{A}}(t)$ per spin [40]. Figure 2 shows that non-zero coupling to the central spin increases the rate of the entanglement growth as:

$$S_{\mathcal{A}} \sim \xi s_{\infty} \left(1 + kA^2 \right) \ln t, \tag{4}$$

where k is a constant that is independent of W and A. Note that the slope of the logarithmic entanglement growth may be completely dominated by the central spin (left inset of Fig. 2). Equation (4) can be rewritten as $S_{\mathcal{A}} = \tilde{\xi}\tilde{s}_{\infty} \ln t$, where $\tilde{\xi}$ and $\tilde{s}_{\infty}$ are the effective correlation length and the saturation entropy density in the presence of the central spin.

The enhancement of the logarithmic entanglement growth originates from an increase in both $\tilde{\xi}$ and $\tilde{s}_{\infty}$ compared to ξ and s_{∞}, as we discuss in the supplementary material [37]. The functional form of the enhancement coincides with the enhancement of fluctuations of magnetization $\mathcal{F}$ between the considered bipartitions. More specifically, for $\mathcal{F} = \left\langle J_{\mathcal{A}}^{z\,2} \right\rangle - \left\langle J_{\mathcal{A}}^{z} \right\rangle^2$ with the total spin $J_{\mathcal{A}}^{z} = \sum_{i\in\mathcal{A}} I_z^i$ inside a bipartition $\mathcal{A}$ for eigenstates in the center of the spectrum, we find the same dependency: $\mathcal{F} \sim kA^2/W^2$ (see right inset of Fig. 2). We emphasize that $\mathcal{F}$ is not extensive in the localized phase [37], such that the total amount of magnetization 'transmitted' through the central spin remains constant if the system size is increased. This critical behavior is necessary for simultaneously maintaining both a constant magnetization exchange and localization at $K \to \infty$. It is a result of the rescaling A/K of the coupling term in Eq. (1). Notably, we have found the same scaling for the logarithmic transport in the NCSM using second order perturbation theory in A. [41] While the similar functional dependence suggests that fluctuations of magnetization are responsible for the enhanced growth of entanglement entropy, analytical understanding of the increase in $\tilde{\xi}$ and $\tilde{s}_{\infty}$ remains an interesting open question.

We conclude that, at sufficient disorder strength, the central spin model is many-body localized in terms of thermodynamical and quantum statistical perspectives. Information, witnessed by entanglement entropy, spreads at most logarithmic in time. Eigenvalues are Poisson-distributed and the corresponding eigenvectors have an area-law entanglement entropy [37]. The system fails to self-thermalize and preserves information about the initial state.

Detecting MBL with the central spin.– After we have demonstrated that there exist systems in which the in-
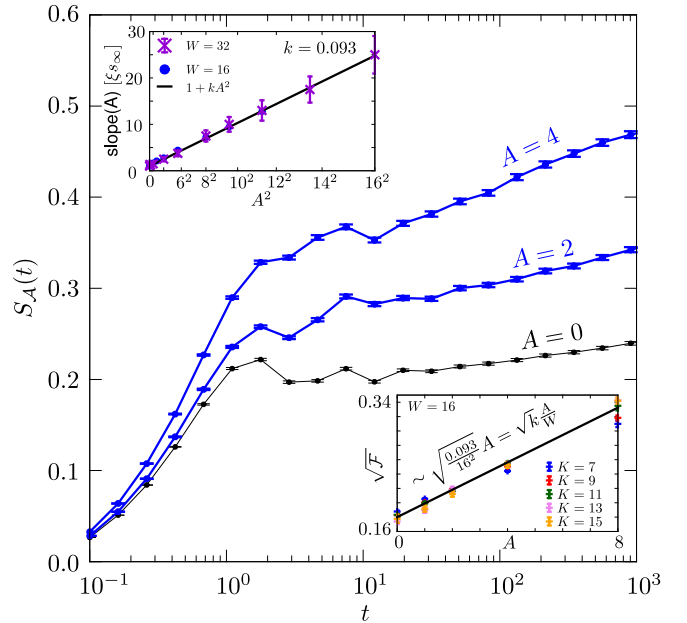

Figure 2. Growth of entanglement entropy $S_{\mathcal{A}}(t)$ of the Néel state for different coupling constants to the central spin. In the localized phase, we find that the slope of the logarithmic entanglement growth increases quadratically with A (see upper left inset), which motivates Eq. (4). For the fit parameter k we find $k \approx 0.093(5)$. The bottom right inset shows the fluctuation $\mathcal{F}$ (see text) of eigenstates inside the localized phase. We find a non-extensive behavior of $\mathcal{F} \sim kA^2/W^2$, which, as $\xi \sim 1/W^2$, traces the enhancement of $S_{\mathcal{A}}(t)$ back to magnetization exchange between bipartitions. The data is generated for $W = 16$ using 14 spins.

sertion of a central spin does not destroy the MBL phase, we explain how the central spin can be used as an ideal (non-demolition) detector of MBL. In particular, we assume that the measurable quantity is a spin component of the central spin, e.g. $S_z(t) = \langle\psi(t)|S_z|\psi(t)\rangle$. We investigate its autocorrelation function

$$
\begin{aligned}
C(t) &= \int_{-\infty}^{\infty} \mathrm{d}\tau \, S_z(t+\tau)S_z(\tau) \\
&= \sum_{nm} \left| \rho_{nm}^E \right|^2 \left| (S_z^E)_{nm} \right|^2 e^{i(E_n - E_m)t},
\end{aligned} \tag{5}
$$

where S_z^E and ρ^E are the observable and the initial density matrix in the energy space of eigenstates with energies E_n, *cf.* [37]. The Fourier transform of Eq. (5) yields

$$
\begin{aligned}
f^2(\omega) &= \frac{1}{2\pi} \int_{-\infty}^{\infty} e^{-i\omega t} C(t) \\
&= \sum_{nm} \left| \rho_{nm}^E \right|^2 \left| (S_z^E)_{nm} \right|^2 \delta[\omega - (E_n - E_m)].
\end{aligned} \tag{6}
$$

Note that $f^2(\omega)$ is frequently studied in the context of the ETH [42] and is thus a natural candiate for helping to identify localization [43]. Evidently, ρ_z^E and S_z^E can only contribute to $f^2(\omega)$ if there exists two energies
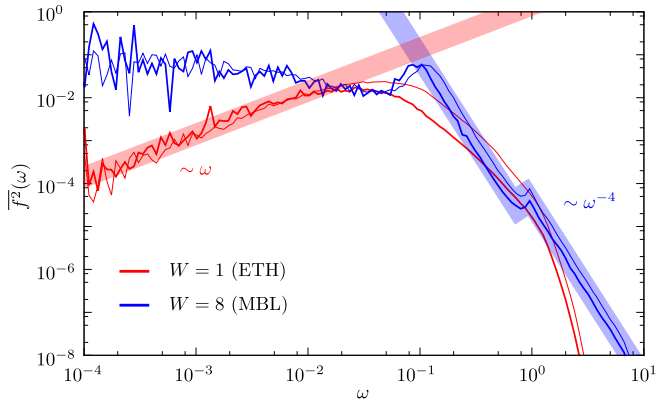
Figure 3. Fourier spectrum of the autocorrelation function. At small frequencies $\omega \ll A$, the central spin can detect the ETH phase (red) by a linear decay of $\overline{f^2}(\omega)$, which originates from level repulsion. In the MBL phase, $\overline{f^2}(\omega)$ shows a significant power-law decay over many orders of magnitude. The exponent -4 is independent of system size, disorder, and coupling strength. The two peaks at $\omega \sim 10^{-1}$ and $\omega \sim 1$ correspond to the local interactions A and A/K, which are revealed in the dynamics of the central spin. Data is generated for 10 (thin lines) and 12 (thick lines) spins at $A = 1$. The colored areas are guides for the eye and indicate the power-law behaviors.

with $\omega = E_i - E_j$ exists. The energies E_i and E_j are not limited to be adjacent energy levels, but yet, the behavior of $f^2(\omega)$ for $\omega \ll \langle \delta_i \rangle$ is dominated by the statistics of level spacings $\delta_i = E_{i+1} - E_i$. In particular, in the ergodic phase, where eigenvalues repel each other, the probability to find a small level spacing behaves as $p(\omega)\mathrm{d}\omega = (\pi/2)\omega e^{-\pi\omega^2/4}\mathrm{d}\omega \propto \omega\mathrm{d}\omega$. Therefore, in contrast to the localized phase, we expect that $f^2(\omega)$ is linearly suppressed in the ergodic phase. The dynamics of the central spin is hence influenced by the level statistics of the surrounding spins. We illustrate this feature in Fig. 3, where we present the disorder average of the smoothed discrete function

$$\overline{f^2}(\omega_i) = \frac{1}{\Delta(\omega_i)} \int_{\omega_i}^{\omega_i + \Delta(\omega_i)} \mathrm{d}\omega \ f^2(\omega). \tag{7}$$

We indeed find $\overline{f^2}(\omega) \sim \omega$ in the extended phase at small frequencies $\omega \ll A/K$.

Above we have demonstrated that the presence or absence of level repulsion manifests in a qualitatively different behavior of $\overline{f^2}(\omega)$ at frequencies of the order of the level spacing, hence allowing to distinguish between MBL and ergodic phases. In addition, we also observe a qualitatively different behavior of the autocorrelation function at larger frequencies. In the MBL phase, we find clear peaks of $\overline{f^2}(\omega)$ at $\omega = 1$ and $\omega = A/K$, corresponding to the coupling strength between neighbored spins of the Heisenberg chain and their coupling strength to the central site, respectively. In that case, the dynamics of the central spin is strongly affected by local interac-

tions, in contrast to the extended phase where we do not see any pronounced features. It should be noted that most weight of $\overline{f^2}(\omega)$ is concentrated in the vicinity of $\omega = A/K$ in the localized phase (this is masked by the logarithmic scale in Fig. 3).

The last and most significant feature is the power-law decay of $\overline{f^2}(\omega)$ in the localized phase for $\omega > A/K$, which ranges (even in our rather small system of 14 spins) over 7 orders of magnitude. A power-law dependence of a related quantity to $f^2(\omega)$ has recently been studied in terms of localization in Ref. [44]. We find that the exponent of the power-law is independent of system size (see Fig. 3), disorder strength, and also independent of the coupling strength to the central spin [37]. Further, for different distributions of random numbers, such as normal and lognormal distributions, we have observed the same exponent $p = -4$, which therefore seems to be a generic exponent of this model and a novel indicator of MBL.

From the experimental side, one possible realization of our model is afforded by nitrogen vacancy (NV) centers in diamond [45, 46]. We envision working with high nitrogen density Type Ib samples, where the dominant defects are spin-$1/2$ P1 centers (nitrogen impurities). In this case, the NV center then plays the role of an optically addressable central spin while the P1 centers play the role of the bath spins. By working at a magnetic field near $B \sim 510$ G, the NV and the P1 defects become resonant and dipolar couplings mediate strong interactions between them [47]. We note that in this setup, disorder occurs also in the strength of these dipolar interactions, which scale as $1/r^3$. Finally, one should be able to directly measure the central NV's frequency dependent spin-spin autocorrelation function. This can be done via spin-echo like pulse sequences in the range $\omega \sim 10^{-1} J$ to $10^2 J$ [46].

Conclusion.—We have studied dynamical and statistical properties of a central spin variant of the Heisenberg model. Using an equal coupling strength A/K to all spins, where K is the length of the Heisenberg chain, the system shows, depending on the disorder strength, either a MBL or ergodic phase. We have identified an analytical function $W_c(A)$ for the critical disorder strength at which the phase transition occurs. In the localized phase, $W > W_c(A)$, we have observed an enhanced logarithmic spreading of entanglement entropy, which induced by a non-extensive exchange of magnetization. We have proposed to employ the central spin as a detector to distinguish between MBL and ergodic phase by means of autocorrelation functions.

[1] P. W. Anderson, Phys. Rev. **109**, 1492 (1958).
[2] D. Basko, I. Aleiner, and B. Altshuler, Ann. Phys. **321**, 1126 (2006).
[3] J. M. Deutsch, Phys. Rev. A **43**, 2046 (1991).
[4] M. Srednicki, Phys. Rev. E **50**, 888 (1994).
[5] E. P. Wigner, Ann. Math. **62**, 548 (1955).
[6] M. Serbyn, Z. Papić, and D. A. Abanin, Phys. Rev. Lett. **111**, 127201 (2013).
[7] D. A. Huse, R. Nandkishore, and V. Oganesyan, Phys. Rev. B **90**, 174202 (2014).
[8] M. V. Berry and M. Tabor, Proc. R. Soc. A **356**, 375 (1977).
[9] D. A. Abanin, E. Altman, I. Bloch, and M. Serbyn, (2018), arXiv:1804.11065.
[10] E. Levi, M. Heyl, I. Lesanovsky, and J. P. Garrahan, Phys. Rev. Lett. **116**, 237203 (2016).
[11] E. van Nieuwenburg, J. Y. Malo, A. Daley, and M. Fischer, Quantum Sci. Technol. **3**, 01LT02 (2018).
[12] A. L. Burin, (2006), arXiv:0611387 [cond-mat].
[13] N. Y. Yao, C. R. Laumann, S. Gopalakrishnan, M. Knap, M. Müller, E. A. Demler, and M. D. Lukin, Phys. Rev. Lett. **113**, 243002 (2014).
[14] R. M. Nandkishore and S. L. Sondhi, Phys. Rev. X **7**, 041021 (2017).
[15] M. Gaudin, J. Phys. France **37**, 1087 (1976).
[16] D. Loss and D. P. DiVincenzo, Phys. Rev. A **57**, 120 (1998).
[17] J. Lages, V. V. Dobrovitski, M. I. Katsnelson, H. A. De Raedt, and B. N. Harmon, Phys. Rev. E **72**, 026225 (2005).
[18] G. S. Uhrig, Phys. Rev. Lett. **98**, 100504 (2007).
[19] B. Lee, W. M. Witzel, and S. Das Sarma, Phys. Rev. Lett. **100**, 160505 (2008).
[20] H. Brox, J. Bergli, and Y. M. Galperin, Phys. Rev. A **85**, 052117 (2012).
[21] W. A. Coish and D. Loss, Phys. Rev. B **70**, 195340 (2004).
[22] J. Fischer, B. Trauzettel, and D. Loss, Phys. Rev. B **80**, 155401 (2009).
[23] R. Hanson, L. P. Kouwenhoven, J. R. Petta, S. Tarucha, and L. M. K. Vandersypen, Rev. Mod. Phys. **79**, 1217 (2007).
[24] F. Jelezko, T. Gaebel, I. Popa, A. Gruber, and J. Wrachtrup, Phys. Rev. Lett. **92**, 076401 (2004).
[25] R. Hanson, O. Gywat, and D. D. Awschalom, Phys. Rev. B **74**, 161203 (2006).
[26] A. Pal and D. A. Huse, Phys. Rev. B **82**, 174411 (2010).
[27] D. J. Luitz, N. Laflorencie, and F. Alet, Phys. Rev. B **91**, 081103 (2015).
[28] D. Hetterich, M. Serbyn, F. Domínguez, F. Pollmann, and B. Trauzettel, Phys. Rev. B **96**, 104203 (2017).
[29] M. Serbyn, M. Knap, S. Gopalakrishnan, Z. Papić, N. Y. Yao, C. R. Laumann, D. A. Abanin, M. D. Lukin, and E. a. Demler, Phys. Rev. Lett. **113**, 1 (2014).
[30] R. Vasseur, S. A. Parameswaran, and J. E. Moore, Phys. Rev. B **91**, 1 (2015).
[31] D. Roy, R. Singh, and R. Moessner, Phys. Rev. B - Condens. Matter Mater. Phys. **92**, 1 (2015).
[32] M. Serbyn and D. A. Abanin, Phys. Rev. B **96**, 1 (2017).
[33] P. Ponte, C. R. Laumann, D. A. Huse, and A. Chandran, Philos. Trans. R. Soc. A **375**, 20160428 (2017).
[34] D. Hetterich, M. Fuchs, and B. Trauzettel, Phys. Rev. B **92**, 155314 (2015).
[35] P. Reimann, Nat. Commun. **7**, 10821 (2016).
[36] V. Oganesyan and D. A. Huse, Phys. Rev. B **75**, 155111 (2007).
[37] See the supporting online material for more details, which includes Refs. [7, 28, 33, 40, 42, 44].
[38] M. Žnidarič, T. Prosen, and P. Prelovšek, Phys. Rev. B **77**, 064426 (2008).
[39] J. H. Bardarson, F. Pollmann, and J. E. Moore, Phys. Rev. Lett. **109**, 017202 (2012).
[40] M. Serbyn, Z. Papić, and D. A. Abanin, Phys. Rev. Lett. **110**, 260601 (2013).
[41] In the NCSM, we have chosen the scaling $A/\sqrt{K}$ and derived the motion of a single fermion, where the relevant process was derived in 2nd order perturbation theory $\sim A^2/K$. In this work, we have $K/2$ particles (Néel state) instead, which is the reason why a different scaling of the coupling strength, i.e. A/K, yields similar results.
[42] M. Srednicki, J. Phys. A. Math. Gen. **32**, 1163 (1999).
[43] L. D'Alessio, Y. Kafri, A. Polkovnikov, and M. Rigol, Adv. Phys. **65**, 239 (2016).
[44] M. Serbyn, Z. Papić, and D. A. Abanin, Phys. Rev. B **96**, 104201 (2017).
[45] M. W. Doherty, N. B. Manson, P. Delaney, F. Jelezko, J. Wrachtrup, and L. C. Hollenberg, Phys. Rep. **528**, 1 (2013).
[46] R. Schirhagl, K. Chang, M. Loretz, and C. L. Degen, Annu. Rev. Phys. Chem. **65**, 83 (2014).
[47] L. T. Hall, P. Kehayias, D. A. Simpson, A. Jarmola, A. Stacey, D. Budker, and L. C. L. Hollenberg, (2015), arXiv:1503.00830.